since 1961

Baltica

*BALTICA Volume 34 Number 1 June 2021: 71–80*
https://doi.org/10.5200/baltica.2021.1.6

# Determination of the Fractal Dimension of the Active Fault Data along the East Anatolian Fault Zone

*Ebru Aydindag Bayrak[1], Pinar Kirci[2]**

Aydindag, E.B., Kirci, P. 2021. Determination of the Fractal Dimension of the Active Fault Data along the East Anatolian Fault Zone. *Baltica*, *34 (1)*, 71–80. Vilnius. ISSN 0067-3064.
Manuscript submitted 20 January 2020 / Accepted 7 January 2021 / Available online 20 June 2021



**Abstract.** The current study has analyzed active fault data along the East Anatolian Fault Zone (EAFZ) applying both manual (classic) and modern versions of the box counting method. The EAFZ active fault dataset used for analysis was taken from the Geoscience Map Viewer and the Drawing Editor from the website of the General Directorate of Mineral Research and Exploration. The study covered an area stretching from Karlıova in the north to Kırıkhan in the south. The fractal analysis of the earthquake surface rupture and the Holocene fault data was performed. Fractal dimensions of the EAFZ active-fault data were calculated for 15 boxes and compared with correlation coefficient values. The calculated fractal dimension values were found to vary with the density of the active-fault data falling into the boxes. The maximum fractal dimension value $D_1$ was determined for Karlıova and its surroundings, which can be associated with the fault density due to the branching geometry.

***Keywords:*** *the box counting method; fractal geometry; fractal analysis; correlation coefficient; earthquake surface rupture*

✉ *Ebru Aydindag Bayrak[1] (ebruaydindag@gmail.com), Department of Engineering Sciences, Istanbul University Cerrahpasa, Istanbul, Turkey, Pinar Kirci[2*] (pinarkirci@uludag.edu.tr) Department of Computer Engineering, Bursa Uludag University, Bursa, Turkey*
**Corresponding author at the Department of Computer Engineering, Bursa Uludag University, Bursa, Turkey. Email: pinarkirci@uludag.edu.tr*

## INTRODUCTION

The concepts of fractal and fractal geometry were framed and first introduced by Mandelbrot in his book "Les objects fractals" (Mandelbrot 1967, 1989). In contrast to Euclidean geometry, which is attributed to classical geometry and actually deals with regular shapes of man-made objects, fractal geometry, according to Mandelbrot, is a new area of geometry dealing with indented, protruding, broken or complex objects and shapes existing in nature (Ufuktepe, Aslan 2001). Fractal geometry is viewed as a method for describing objects that exist in nature (Ürey 2006). The emergence of the fractal geometry concept was induced by the inadequacy of Euclidean geometry to describe natural phenomena.

One of the first comprehensive studies on fractal analysis was authored by Turcotte (1989). It covered a range of fractal-related topics, explained various terms and concepts, e.g., fractal and fractal dimension, relationship between fractal fragmentation and seismology, and also described methods for determining fractal dimensions. The study (Hirata 1989) into fault systems in Japan, which was performed using the fractal analysis method, represents one of the important study examples reported in geophysics literature. The study by Okubo, Aki (1987) focused on the San Andreas fault system located between the North Gabilan Range and the Salton Sea. The authors used circles to cover the fault traces in the San Andreas fault system for determining fractal dimensions. The study area was divided into six sections, which were

30 km wide and approximately equal in length. The spatial distribution of earthquakes was presumed to be related to the complexity of the fault geometry. Aviles *et al*. (1987) applied fractal analysis to examine characteristic segments of the San Andreas Fault. They measured the fault length using a ruler size method and calculated its fractal dimension values. Although the fault zone was divided into several sub-faults, they characterized the complexity only of the main fault trace. As in the study by Okubo, Aki (1987), the study area was divided into six segments and their fractal dimensions were found to range from 1.0008 to 1.0191. Huang, Turcotte (1990), showed the relationship between the deformation of the Earth's crust and the fault to be chaotic. In the study by Matsumoto *et al*. (1992), fractal analysis was used to assess dimensions of active fault systems in Japan (the Median Tectonic Line, earthquakes on the Izu and Unzen islands) and in the Philippines. In their study, the authors followed the method used by Okubo, Aki (1987). The fractal dimensions estimated along the Median Tectonic Line were found to vary from 1.00 to 1.40. The highest fractal dimension (1.40), which was calculated for the Unzen area, was attributed to the complexity of the fault system (Matsumoto *et al*. 1992). In the study by Idziak, Teper (1996), the fractal dimensions of the examined fault system above the Silesian coal mine basin in Poland were calculated using the box counting method. In Japan, fractal structures of three geological systems (i.e., epicenters of fault activity, and spatial distribution of rivers) were studied. Fractal dimensions of geological systems were calculated employing the box counting method in the study by Lei, Kusunose 1999. In Japan, the box counting method was used to determine the relationship between the spatial distribution of shocks and fractal dimensions of the fracture system (Nanjo, Nagahama 2000). The same technique was used to calculate fractal dimensions of Gujarat, India, in the study by Ram, Roy (2005), where the area was divided into five blocks and fractal dimensions were estimated for each of them. In that study, the Kachchh rift block was found to have the lowest fractal dimension. The box counting method was employed to calculate fractal dimensions of active faults in the Indian landmass using the MATLAB program. The fractal dimensions of the study area were found to vary from 1 to 1.25 (Jaya *et al*. 2014). In recent years, the complexity of the fault systems and the impact of branching geometry along fault zones have become evident (Scholz *et al*. 2010).

In the study by Ceylan (2006), fractal properties of earthquakes in the Marmara Sea region were studied based on the 1975–2005 earthquake data. The author calculated the capacity dimension $D_0$, information dimension $D_1$ and correlation dimension $D_2$. The fractal dimensions calculated for the entire system were $D_0 = 1.59$, $D_1 = 1.56$ and $D_2 = 1.51$ (Ceylan 2006). A fractal-based model was developed and proposed as an intermediate-term forecasting tool for determining locations of the expected earthquakes in the East Anatolian fault system. Four different methods, i.e., least square regression, least sum of absolute deviation regression, orthogonal regression and robust regression, were employed in the study. To ensure that analysis is comprehensive, the East Anatolian region was divided into 19 different seismotectonic segments (Öztürk 2015). In this study into the San Andreas and North Anatolian fault zones, Aydindag (2015) also used the box counting method and fractal dimension analysis. The author split the study area into multiple boxes with the side length of 30-km. The fractal dimension values calculated for these fault segments ranged approximately from 0.9 to 1.50. Regional and temporal characteristics of seismicity in East Anatolia were studied in (Öztürk 2018). The correlation between the fractal dimension $D_c$ and Gutenberg Richter *b*-value was revealed. Also, *Z*-value was used to determine recent variations in seismic activity.

The aim of this study was to explain the irregularity of the faults in the East Anatolian Fault Zone (EAFZ) using fractal geometry.

## EAST ANATOLIAN FAULT ZONE

The East Anatolian Fault Zone begins at the triple junction of the North Anatolian Fault Zone, Karlıova, and the Ölü Deniz Fault System in the southwest. The length of the East Anatolian Fault zone is 580 km, and its strike direction is northeast-southwest. The East Anatolian Fault zone consists of 6 segments. It has a left lateral strike slip fault system (Kartal, Kadirioğlu 2013).

Four types of active faults are recorded in Turkey. In the active faults database (Geoscience Map Viewer and Drawing Editor), they are referred to as: 1) faults with earthquake surface rupture; 2) Holocene faults; 3) Quaternary faults, and 4) probable Quaternary faults or lineaments.

Faults with earthquake surface rupture have been generating large-magnitude earthquakes since AD 1900. There are reliable data on the location and the total length of the surface rupture. The Holocene fault evinces that the surface rupture dates from the Holocene time (last 11.000 years) (Emre *et al*. 2018).

In this study, the fractal analysis of the data on the above-mentioned faults with earthquake surface rupture and the Holocene fault have been performed (Fig. 1). The Google Earth images of the 15 boxed segments of the East Anatolian Fault Zone were examined (Fig. 2). The study area stretched from Karlıova in the north to Kırıkhan in the south. Given that each

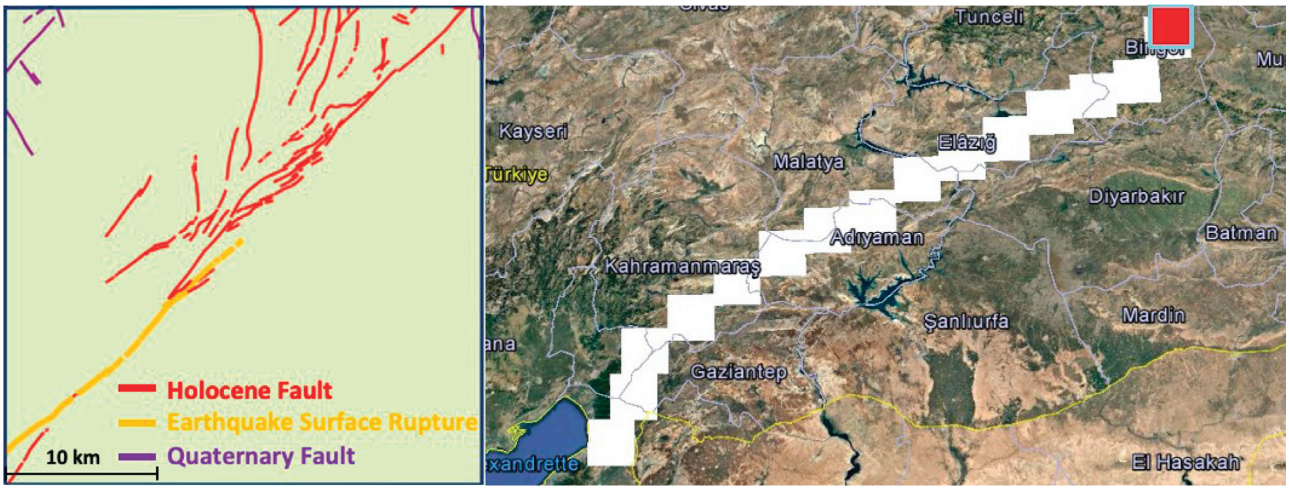


**Fig. 1** Fractal analysis of fault areas along the East Anatolian Fault Zone (based on the website of the General Directorate of Mineral Research and Exploration)

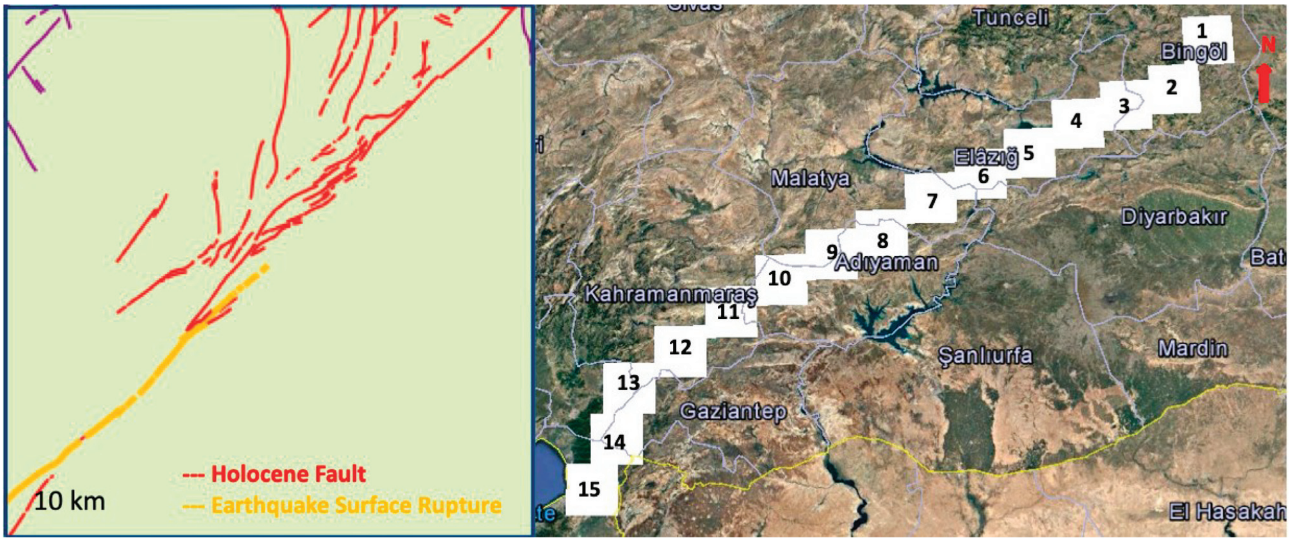


**Fig. 2** The Google Earth image showing the boxed segments along the East Anatolian Fault Zone (EAFZ) (based on the website of the General Directorate of Mineral Research and Exploration)

of the 15 study segments was 30 km long, the total length of the fault zone was 450 km (15 × 30 km) and its total area was 13.500 km$^2$. The active-fault dataset for EAFZ was taken from the Geoscience Map Viewer and Drawing Editor from the website of the General Directorate of Mineral Research and Exploration (Geoscience Map Viewer and Drawing Editor).

Figure 1 shows the active fault data based on the Geoscience Map Viewer and Drawing Editor (Holocene Fault, Fault with Earthquake Surface Rupture and Quaternary Fault). The Google Earth image shows the boxed fault segments in the East Anatolian Fault Zone that were subjected to fractal analysis. To enable the application of the box counting method, the boxes were laid out over the image of the study area so that the main fault lines would run through the box centers.

## BOX COUNTING METHOD

The box counting method involves covering a spatial dataset (object or image etc.) with a grid of boxes of different side length (r) and counting the number of boxes (N) required to do this for each different box side length. The relationship between the box size and the number of boxes required to cover an object is used to calculate the fractal dimension (Turcotte 1989). At every iteration, the size of each box is divided into smaller parts/pieces. The dataset may be composed of points, lines, or higher-dimensional shapes. Boxes are used to encompass the data, the shape of the boxes being mostly square. To predict a fractal dimension, the data are grouped into different-sized boxes multiple times. Employing the box counting method, D is calculated by using Equation 1 as follows:

$$D = \lim_{r \to 0} \frac{\log(N(r))}{\log(1/r)} \quad (1)$$

where N(r) is the number of boxes containing data and r is the side length of the boxes. Log (N(r)) versus log((1/r)) is used to find the fractal dimension (D) as r approaches zero, as shown in Fig. 3. The graph is plotted as a straight line and the slope is equal to the fractal dimension. In (Gonzato 1998) and (Bourke 2014), an algorithm was developed to calculate the fractal dimension using the box counting method.

The box counting procedure consists of the following steps:

Step 1. The image of the fault area is overlaid with boxes whose side length is r. Then, the boxes containing the fault data is counted.

Step 2. The side length (r) of the box is divided by two. The resulting side length is r/2, and the boxes containing fault data is counted.

Step 3. The obtained side length (r/2) of the boxes is divided by two, and the side length becomes r/4. Then, again, the boxes containing fault data are counted.

Log N (r) - Log 1/r is represented by a statistical flat curve in Cartesian coordinates, and the slope of this curve indicates the fractal dimension value (Aydındağ 2015).

## MANUAL APPLICATION OF BOX COUNTING METHOD

The active fault data along the East Anatolian Fault Zone (EAFZ) were subjected to fractal analysis, which was carried out applying the box counting method. In this study, the box counting method was applied manually, and the effect of the human factor was maintained at the lowest level as shown in Fig. 4. The determined size of the first box was 30 km × 30 km and the examined EAFZ area was split into 15 boxed segments in total. The boxes were laid out over the image of the study area so that the main fault line would run through the center of the boxes. The manual box counting method was applied following a 5-step procedure.

On every step of the algorithm application procedure, the side length of the boxes was reduced and the active fault data falling into the boxes increased accordingly.

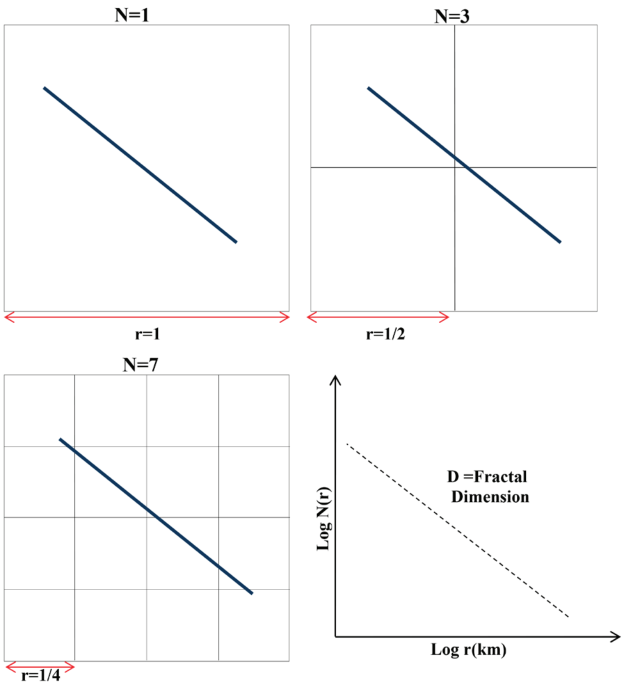


**Fig. 3** Simplified representation of the box counting method application (Aydındağ et al. 2018)

## MODERN VERSION OF THE BOX COUNTING METHOD USING THE FRACTALYSE IMAGE ANALYSIS SOFTWARE

The Fractalyse Image Analysis Software was used to enable the application of the box counting method for analyzing the EAFZ active fault data. The aforementioned image analysis program was developed by the research team of the Thema Research Center at Franche-Comte University in collaboration with the French National Center for Scientific Research (Fractalyse Analysis Software).

To carry out the fractal analysis of the active fault data, the boxes were arranged as described in the section under the heading "The East Anatolian Fault Zone". As the working principle of the Fractalyse image analysis software is based on the black-and-white format, the fault data were processed using the image analysis program and converted into the black-and-white format (the background should be white and active fault data black). Furthermore, the Tiff (Tagged Image File Format) image format or Bmp (Bitmap) extension should be used as shown in Fig. 5.

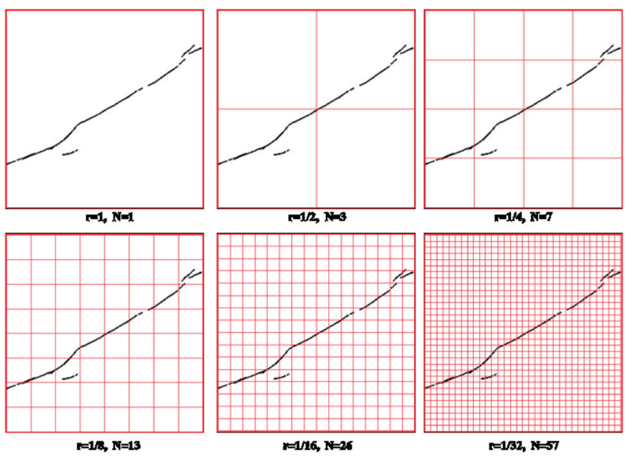


**Fig. 4** The manual (classic) application of the box counting method

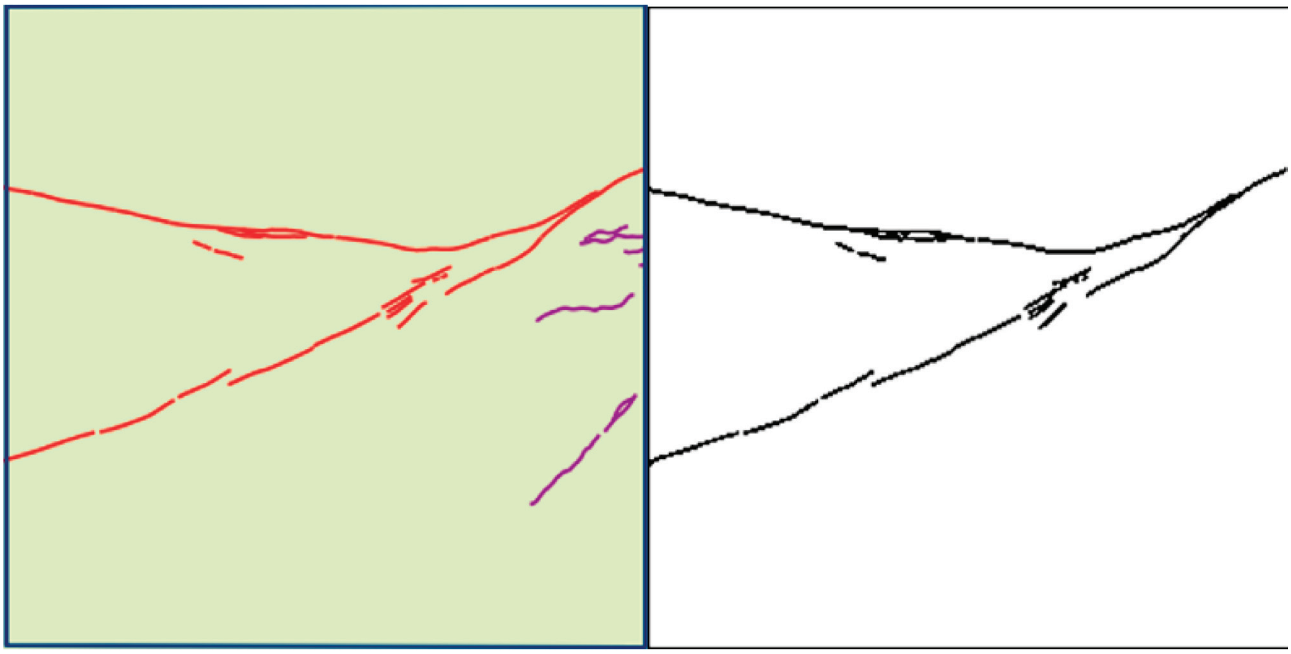

**Fig. 5** The image of EAFZ converted into the black-and-white format for the modern application (based on the website General Directorate of Mineral Research and Exploration)

The images of the East Anatolian Fault Zone (Geoscience Map Viewer and Drawing Editor) were converted into the black- and-white format to enable the application of the modern version of the box counting method as illustrated in Fig. 5. Data on the fault with earthquake surface rupture and on the Holocene fault were also subjected to fractal analysis (Geoscience Map Viewer and Drawing Editor).

To perform fractal analysis, the numbers of the counted black pixels and the box side lengths were marked in the Cartesian coordinate system, where X-axis represented box side lengths, and Y-axis represented the number of the counted black pixels. The fractal dimension was calculated from the slope of the curve, which showed the relationship between the number of the counted black pixels in the fault image and the box side lengths. The fractal size values of each boxed area were computed applying both the Grid and the Free box methods. However, the fractal size values of each boxed area computed applying these methods differed. The Grid method is the most commonly used method for estimating fractal dimensions. When using the Grid method, the image of the study area was covered with a quadratic grid and then the grid distance $\varepsilon$ was modified. Following the earlier described logic, for each value of $\varepsilon$, the number of squares $N(\varepsilon)$ containing fault-related pixels was counted. In the case of the Free box method, the number of boxes containing black data pixels is required to be minimal. The algorithm converged on the minimum in infinite time, so the results obtained were only an approximation of the optimal coverage.

## RESULTS

The active fault data along the East Anatolian Fault Zone were investigated applying the box counting method, which is the most popular among fractal analysis methods. In the study, the grid of boxes was laid out over the image of the faults passing through the centers of the main areas. Other faults (secondary faults) passing through the data analysis boxes were also included in the analysis. The computation of fractal dimension values of the fifteen 30 × 30-km-sized boxes spanning the area of the fault zone using the box counting method yielded different results. Therefore, the fractal analysis of the active fault data was carried out employing both versions of the box counting method, i.e., the manual and the modern one.

The fractal dimensions of the main EAFZ fault trace calculated applying the manual version of the box counting method were found to vary between 0.81 and 1.47. One of the highest EAFZ fractal dimension values computed employing this version of the box counting method was obtained for the Bingöl-Center as shown in Fig. 6.

Figure 6 presents the fractal dimension and the regression coefficient of determination (on the right) for Bingöl-Center, Çayboyu, which were determined applying the manual version of the box counting method. The fractal dimension value of this fault segment was the second highest because the data falling into the box exhibited high intensity.

The lowest fractal dimension value (0.81) was obtained for the area of Hazar Lake and its surroundings

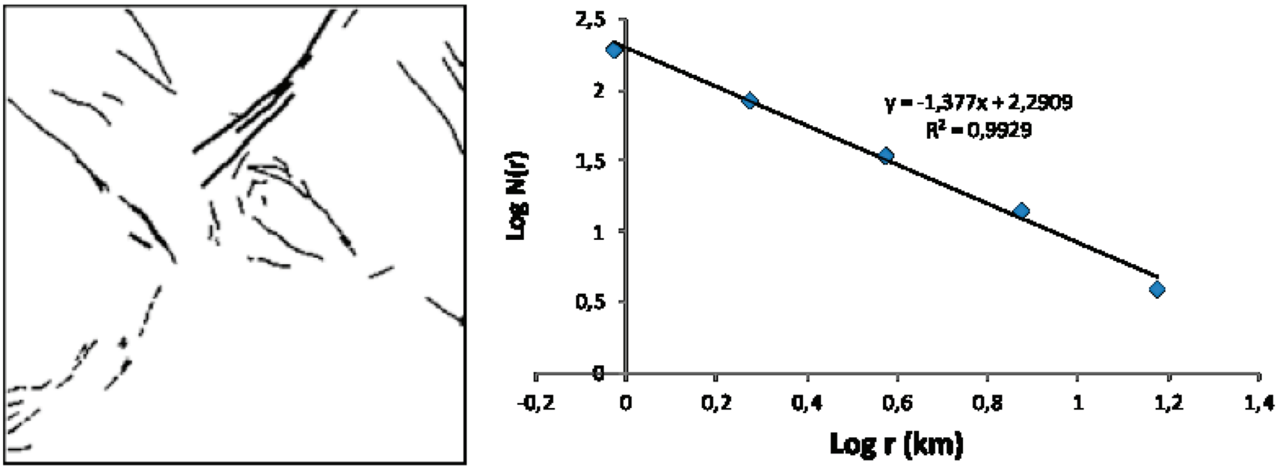


**Fig. 6** The manual application of the box counting method (Bingöl-Center, Çayboyu)

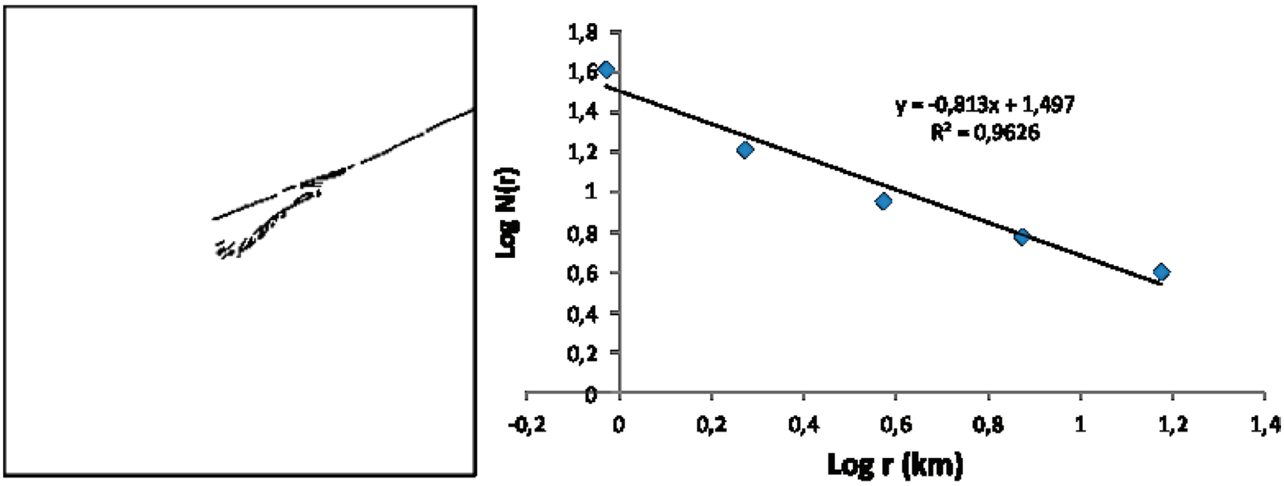


**Fig. 7** The smallest fractal dimension value was obtained for the boxed area of Hazar Lake and its surroundings. The manual version of the box counting method was applied

enclosed in Box 5, which is explained by the sparsity of the data falling into this box, i.e., the area enclosed in Box 5 is occupied by Hazar Lake with no fault line extension (Fig. 7).

When using the manual version of the box counting method, the smallest fractal dimension value was obtained for the box encompassing Hazar Lake and its surroundings. The fractal dimension value and the regression coefficient of determination are shown on the right.

The modern version of the box counting method is represented by the Free box and Grid methods, which were implemented using the Fractalyse image analysis software. The application procedure of the modern version of the box counting method, just like that of the manual version, consists of 5 steps.

In this study, Free box and Grid methods were applied separately to characterize 15 boxed segments of the East Anatolian Fault Zone. The fractal dimension values of the 15 EAFZ boxed segments calculated using the Free box method ranged from 0.78 to 1.25. The analysis of the same 15 EAFZ boxed segments employing the Grid method provided similar results, i.e., the fractal dimension values were found to range from 0.83 to 1.31.

The results obtained using the Grid method are shown in Figs 8 and 9. The fractal dimension value $D_1$ and the correlation coefficient of the area (Box 1) covering Karlıova and its surroundings computed applying the Grid method were 1.3100 and 0.9991, respectively. The lowest fractal dimension value ($D_7$ = 0.83) was calculated for the Malatya-Pütürge area enclosed in Box 7.

Figure 8 illustrates the application of the Grid method to the Bingöl-Karlıova region. The fractal dimension value and the correlation coefficient are presented.

Figure 9 illustrates the application of the Grid method to the Malatya-Pütürge region. The fractal dimension and correlation coefficient are presented.

Figs 10 and 11 show the results of the East Anatolian Fault Zone fractal analysis obtained applying

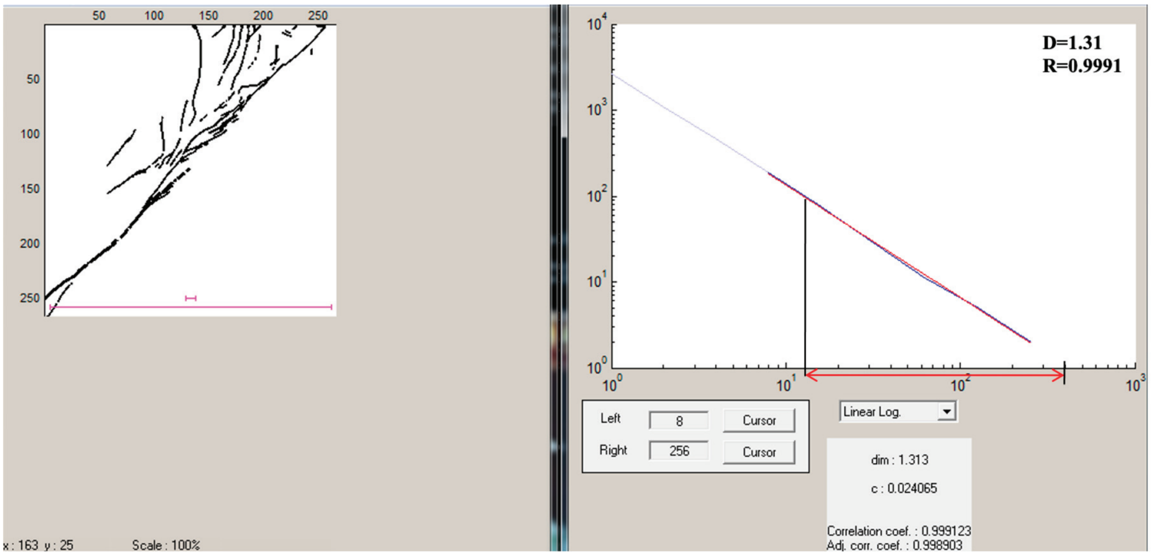


**Fig. 8** The Grid method application (Bingöl-Karlıova)

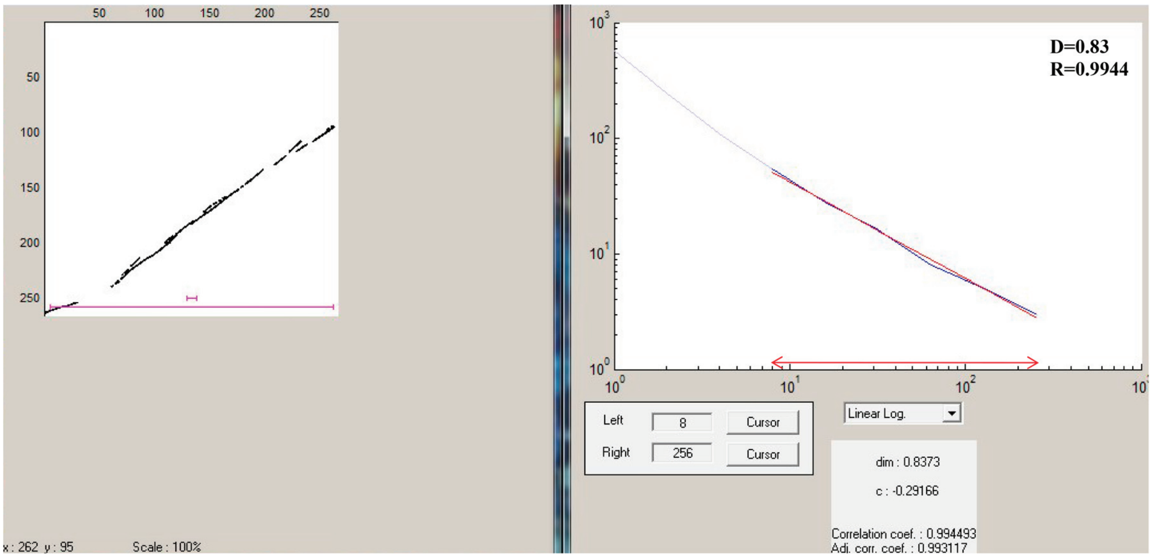


**Fig. 9** The Grid method application (Malatya-Pütürge)

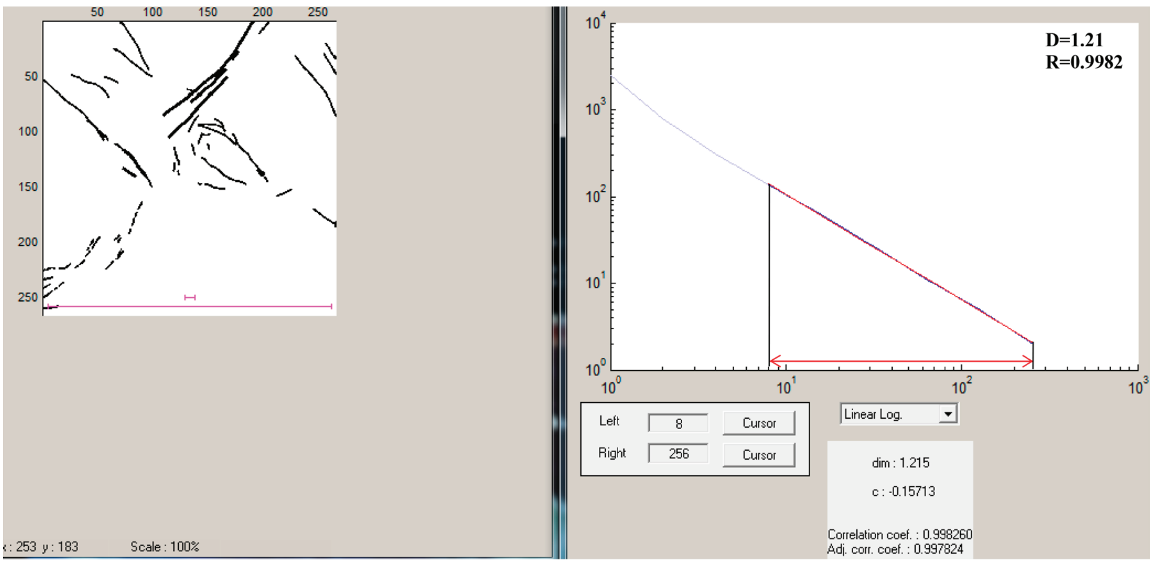


**Fig. 10** The Free box method application (Bingöl-Center)

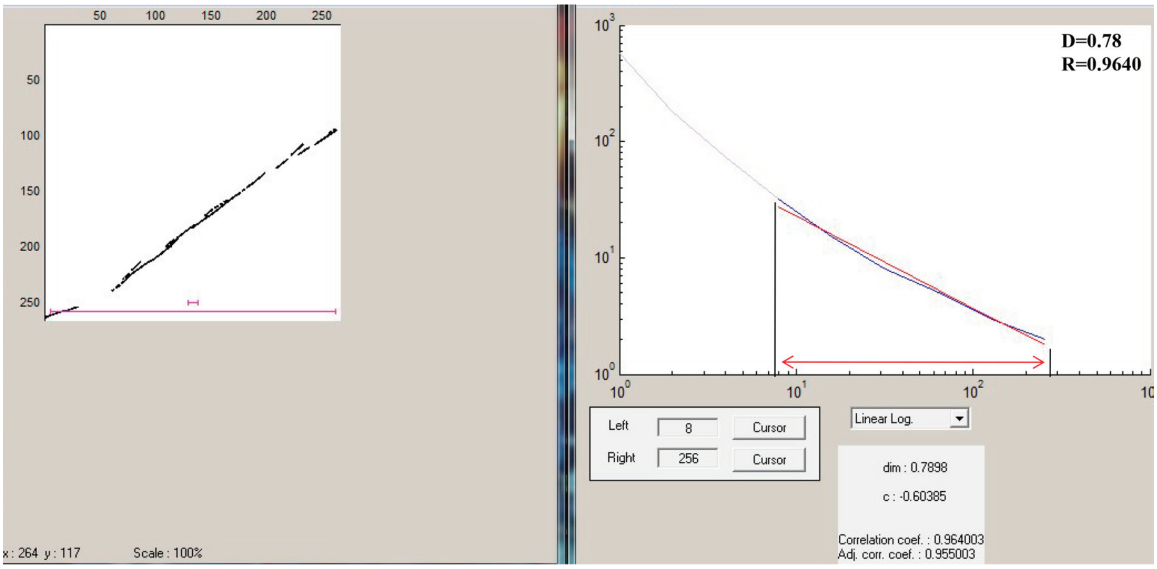


**Fig. 11** The Free box method application (Malatya-Pütürge)

the Free box method. The Bingöl-Center area shows the highest correlation coefficient R = 0.9982 and the fractal dimension value 1.21. The lowest fractal dimension value calculated using the Grid method was obtained for the Malatya-Pütürge area.

Figure 10 shows the application of the Free box method to the Bingöl-Center region as well as values of the fractal dimension and correlation coefficient.

Figure 11 illustrates the application of the Free box method to the Malatya-Pütürge region and presents values of the fractal dimension and correlation coefficient. The fractal dimension values of the active fault segments in the East Anatolian Fault Zone computed applying different fractal analysis methods, i.e., the manual and the modern automated version, differed. The correlation coefficient (R) of all the boxed areas computed using the box counting method was found to be statistically high (R > 0.9). The fractal dimension values of the EAFZ determined applying the manual and the modern versions of the fractal analysis method are shown in Table 1 and Table 2, respectively. Since the correlation coefficient is close to 1, the relationship between the two variables is strong, positive.

The performed analysis of fractal properties of the active fault data using the manual box counting method and its modern versions has made it possible to express fault irregularities in fault areas in the East Anatolian Fault Zone mathematically. The obtained high fractal dimension can be linked to the fragmented and irregular geometry of the fault in that

**Table 1** The fractal dimension values and correlation coefficients, which were determined for each boxed segment of the EAFZ employing the manual version box counting method

| The box number | Fractal Dimension | Correlation Coefficient |
|---|---|---|
| $D_1$ | 1.47 | 0.9999 |
| $D_2$ | 1.37 | 0.9964 |
| $D_3$ | 1.19 | 0.9993 |
| $D_4$ | 1.05 | 0.9991 |
| $D_5$ | 0.81 | 0.9811 |
| $D_6$ | 1.02 | 0.9989 |
| $D_7$ | 1.01 | 0.9979 |
| $D_8$ | 1.21 | 0.9986 |
| $D_9$ | 1.12 | 0.9976 |
| $D_{10}$ | 1.02 | 0.9985 |
| $D_{11}$ | 1.21 | 0.9987 |
| $D_{12}$ | 1.15 | 0.9997 |
| $D_{13}$ | 1.02 | 0.9986 |
| $D_{14}$ | 1.20 | 0.9967 |
| $D_{15}$ | 1.15 | 0.9998 |

**Table 2** Fractal dimension values and correlation coefficients of each boxed EAFZ area determined employing the Free box and the Grid methods

| The box number | Fractal Dimension Grid | Correlation Coefficient (Grid) | Fractal Dimension (Free box) | Correlation Coefficient (Free box) |
|---|---|---|---|---|
| $D_1$ | 1.31 | 0.9991 | 1.25 | 0.9812 |
| $D_2$ | 1.23 | 0.9994 | 1.21 | 0.9982 |
| $D_3$ | 1.15 | 0.9972 | 1.09 | 0.9978 |
| $D_4$ | 0.98 | 0.9969 | 0.86 | 0.9838 |
| $D_5$ | 0.83 | 0.9383 | 0.94 | 0.9591 |
| $D_6$ | 1.11 | 0.9922 | 1.02 | 0.9993 |
| $D_7$ | 0.83 | 0.9944 | 0.78 | 0.9640 |
| $D_8$ | 1.10 | 0.9959 | 1.00 | 0.9783 |
| $D_9$ | 1.10 | 0.9985 | 1.04 | 0.9947 |
| $D_{10}$ | 0.90 | 0.9938 | 0.90 | 0.9956 |
| $D_{11}$ | 1.13 | 0.9975 | 1.02 | 0.9718 |
| $D_{12}$ | 1.01 | 0.9925 | 1.01 | 0.9980 |
| $D_{13}$ | 0.89 | 0.9888 | 0.87 | 0.9868 |
| $D_{14}$ | 0.96 | 0.9939 | 0.97 | 0.9939 |
| $D_{15}$ | 1.13 | 0.9953 | 1.04 | 0.9959 |

region. The maximum values of the fractal dimension can be correlated with the fault density attributable to the branching geometry. On the other hand, the low value of the fractal dimension can be explained by the linear and simple geometry of the fault.

## CONCLUSION

The East Anatolian Fault Zone (EAFZ) was investigated applying the box counting method. The box size was 30 km × 30 km. The performed fractal analysis of EAFZ showed that the total fault length is 450 km (15 × 30 km) and the fault area is 13,500 km$^2$. Data on the faults with earthquake surface rupture and the Holocene fault were based on the active fault database of Turkey. The fractal analysis of EAFZ performed applying the manual and the modern versions of the box counting method yielded different fractal dimension values.

The highest fractal dimension value was obtained for $D_1$ (Box 1) covering the Karlıova region and its surroundings. It can be explained by the fault density due to the branching of the rupture zone. Karlıova is located at the intersection point of several fault zones, i.e., East Anatolia, Northeast Anatolia and North Anatolia. Therefore, Karlıova is sometimes called a triple junction. When using the manual version of the method, the lowest fractal dimension value (0.81) was determined for $D_5$ (Box 5), which covers Hazar Lake and its surroundings. However, when the modern Free Box and Grid methods were applied, the lowest fractal dimensions (0.78 and 0.83 respectively) were obtained for Pütürge and its surroundings. The lowest fractal dimension value calculated for this region is attributable to the fault data sparsity therein.

It should be emphasized that the current study of the EAFZ is limited to the currently available dataset and the values presented here are likely to change with the data quality improvement. Further research should focus on the fractal analysis of historical earthquakes, where the influence of lithological trends can be incorporated. Future studies of EAFZ should also include geothermal resources and areas with mineral resource potential. Analysis of plate velocity changes and earthquake clusters is likely to provide additional insights.


## ACKNOWLEDGMENTS

The authors express sincere thanks to two anonymous reviewers for their constructive comments and suggestions that have greatly improved the quality of the manuscript.


## REFERENCES


Aviles, C.A., Scholz, C.H., Boatwright, J. 1987. Fractal analysis applied to characteristic segments of the San Andreas fault. *Journal of Geophysical Research: Solid Earth 92 (B1)*, 331–344.

Aydındağ, E. 2015. *Kuzey Anadolu ve San Andreas Fay Zonlarında Aktif Fay Verilerinin Fraktal Analizi,* İstanbul University, MSc Thesis, 115. [In Turkish].

Aydındağ, E., Kırcı, P., Kırbaşlar, İ. 2018. Fractal Analyzing of Active Earthquake Fault Data in the Eastern Anatolian Fault Zone. In: *2018 IEEE First International Conference on System Analysis & Intelligent Computing (SAIC)*. IEEE, 1–3.

Bourke, P. 2014. Box counting fractal dimension of volumetric data. http://paulbourke.net/fractals/cubecount/

Ceylan, S. 2006. Fractal properties of earthquakes in Marmara. *Journal of Istanbul Kültür University 4 (3)*, 147–154.

Emre, Ö., Duman, T.Y., Özalp, S., Şaroğlu, F., Olgun, Ş., Elmacı, H., Çan, T. 2018. Active fault database of Turkey. *Bulletin of Earthquake Engineering 16 (8),* 3229–3275.

Gonzato, G. 1998. A practical implementation of the box counting algorithm. *Computers & Geosciences 24 (1),* 95–100.

Hirata, T. 1989. Fractal dimension of fault systems in Japan: Fractal structure in rock fracture geometry at various scales. In: *Fractals in geophysics,* 157–170. Birkhäuser, Basel.

Huang, J., Turcotte, D.L. 1990. Are earthquakes an example of deterministic chaos? *Geophysical Research Letters 17 (3)*, 223–226.

Idziak, A., Teper, L. 1996. Fractal dimension of faults network in the upper Silesian coal basin (Poland): Preliminary studies. *Pure and applied geophysics 147 (2)*, 239–247.

Jaya, V., Raghukanth, S.T.G., Sonika Mohan, S. 2014. Estimating fractal dimension of lineaments using box counting method for the Indian landmass. *Geocarto International 29 (3),* 314–331.

Kartal, R.F., Kadirioğlu, F.T. 2013. Doğu Anadolu Fayının Sismotektoniği ve Bu Fay Üzerindeki Son Beş Yıllık Deprem Aktivitesinin İstatistiksel Analizi, *66. Türkiye Jeoloji Kurultayı* 01–05 Nisan 2013, ODTÜ Kültür ve Kongre Merkezi, Ankara. [In Turkish].

Lei, X., Kusunose, K. 1999. Fractal structure and characteristic scale in the distributions of earthquake epicentres, active faults and rivers in Japan. *Geophysical Journal International 139 (3)*, 754–762.

Mandelbrot, B. 1967. How long is the coast of Britain? Statistical self-similarity and fractional dimension. *Science 156 (3775)*, 636–638.

Mandelbrot, B. B. 1989. Fractal geometry: what is it, and what does it do? *Proceedings of the Royal Society of London. A. Mathematical and Physical Sciences 423 (1864)*, 3–16.

Matsumoto, N., Yomogida, K., Honda, S. 1992. Fractal analysis of fault systems in Japan and the Philippines. *Geophysical Research Letters 19 (4)*: 357–360.

Nanjo, K., Nagahama, H. 2000. Spatial distribution of aftershocks and the fractal structure of active fault systems. In: *Fractals and Dynamic Systems in Geoscience*, 575–588. Birkhäuser, Basel.

Okubo, P.G., Aki, K. 1987. Fractal geometry in the San Andreas fault system. *Journal of Geophysical Research: Solid Earth 92 (B1)*, 345–355.

Öztürk, S. 2015. Depremselliğin Fraktal Boyutu ve Beklenen Güçlü Depremlerin Orta Vadede Bölgesel Olarak Tahmini Üzerine Bir Modelleme: Doğu Anadolu Bölgesi, Türkiye. *Gümüşhane Üniversitesi Fen Bilimleri Enstitüsü Dergisi 5 (1)*, 1–23. [In Turkish].

Öztürk, S. 2018. Earthquake hazard potential in the Eastern Anatolian Region of Turkey: seismotectonic b and Dc-values and precursory quiescence Z-value. *Frontiers of Earth Science 12 (1)*, 215–236.

Ram, A., Roy, P.N.S. 2005. Fractal dimensions of blocks using a box-counting technique for the 2001 Bhuj earthquake, Gujarat, India. *Pure and applied geophysics 162 (3),* 531–548.

Scholz, C.H., Ando, R., Shaw, B.E. 2010. The mechanics of first order splay faulting: The strike-slip case. *Journal of Structural Geology 32 (1)*, 118–126.

Turcotte, D.L. 1986. Fractals and fragmentation. *Journal of Geophysical Research: Solid Earth 91 (B2),* 1921–1926.

Turcotte, D.L. 1989. Fractals in geology and geophysics. *Pure and applied Geophysics 131 (1–2),* 171–196.

Ufuktepe, Ü., Aslan, İ. 2001. *Fraktal Geometri'den Bir Kesit, Matematik Dünyası*, C:11, S:1. [In Turkish].

Ürey, H. 2006. Fraktal Geometri ve Uygulamaları. MSc Thesis. Afyon Kocatepe University, 84. [In Turkish].

**Internet sources**

Geoscience Map Viewer and Drawing Editor: http://yerbilimleri.mta.gov.tr/anasayfa.aspx. Accessed 26 September 2018.

Fractalyse Analysis Software: http://www.fractalyse.org Accessed 15 September 2020.